SOLAR FORCING OF DROUGHT DETECTED IN SNOWFALL RECORDS OF THE CENTRAL SIERRA NEVADA, WESTERN UNITED STATES

John A. Kleppe[1] and Daniel S. Brothers[2]

ABSTRACT

This paper presents wavelet analyses of snow water equivalent (SWE) data from three sites near to the Lake Tahoe Basin (Lake Lucille, Ward Creek, and Mt. Rose) with continuous measurement records since 1910; and a fourth site which is ~180 km to the south at Mammoth Pass with records back to 1928. The correlation amongst the four stations is surprisingly high (0.88), which suggests SWE variation is regionally correlated and that each of these sites experiences the same forcing function. When the International Sunspot Number (ISSN) data are modified to account for magnetic polarity of the sunspots to reflect the reversal of the magnetic field of the sun every ~11 years, the modified ISSN series can be demodulated using suppressed carrier amplitude modulation methods and correlated to the 100 year SWE series. Based on the results presented in this paper, we propose the major driving forces of winter precipitation, in the form of snow, in the northern and central Sierra are the reversal of the sun's magnetic field and a statistically independent "carrier" signal being generated by the Earth's atmospheric circulation parameters including orbital (inclination, eccentricity, precession, obliquity, and rotational), depth of the atmosphere, and heating by the sun. (KEYWORDS: snowpack, sunspots, solar magnetic reversal, rotational, cosmic)

INTRODUCTION

The economies of both California and Nevada are heavily dependent on the annual water supply generated and stored in the snowpack of the Sierra Nevada mountain range Figure 1.

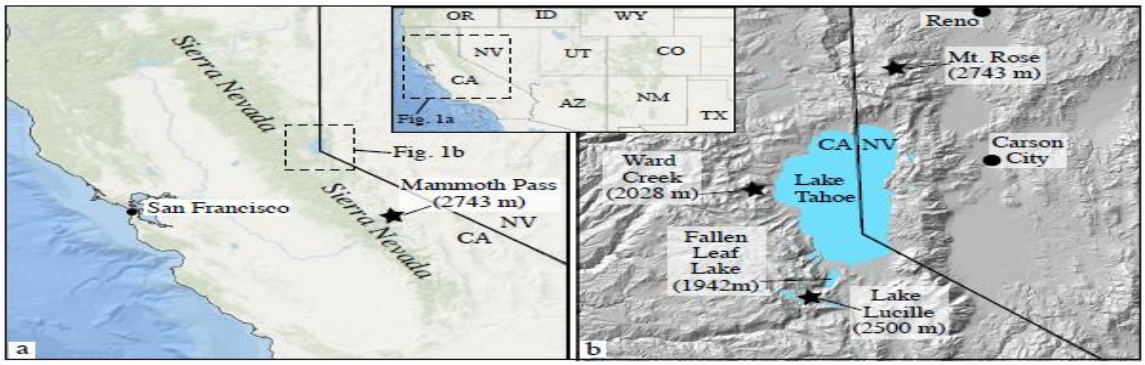

Figure 1. (a) Regional setting, (b) Enlarged map of the Lake Tahoe Basin and surrounding terrain. Snow water equivalent sites (SWE) are labeled as black stars.

Snowpack in the Sierra region provides a natural form of water storage. There are many diverse and sometimes conflicting interests in the understanding, measurement, prediction, management, allocation, and maintenance of this most valuable Sierra Nevada water resource. However, given the recent period of drought, it is now imperative that new water management strategies be developed to account for the potential periodicity of prolonged droughts. To do this requires a better understanding of the main drivers of the precipitation as well as the timing and water storage component of the annual Sierra Nevada snowpack. Because of the sensitivity of FLL to regional drought conditions, we decided to study in more detail the nature and source of the precipitation falling into the FLL basin and surrounding watershed. The goal being to use the FLL watershed as a case study that can be expanded upon to gain a better understanding of the major drivers of precipitation and drought throughout the Sierra Nevada. In this paper, we apply wavelet analysis to SWE time series data at a series of sites near the crest of the

Paper presented Western Snow Conference 2017
[1]John A. Kleppe, College of Engineering, University of Nevada, Reno, NV 89557-0260
[2]Daniel S. Brothers, Pacific Coastal and Marine Science Center, U.S. Geological Survey, Santa Cruz, CA.95060

Sierra Nevada and propose the spectral content of the SWE data can be closely modeled using a simple suppressed carrier amplitude modulation process between the sun's magnetic activity (indicated by sunspots) and a statistically independent "carrier" signal being generated by the Earth's atmospheric circulation parameters including orbital (inclination, eccentricity, precession, obliquity, and rotational), depth of the atmosphere, and heating by the sun.

Ocean Atmospheric Interactions and Formation of the Sierra Nevada Snowpack

There are several ocean-atmospheric interactions normally considered when looking at origins of precipitation forming the Sierra Nevada snowpack including, the Pacific/North American teleconnection pattern (PNA), the El Niño–Southern Oscillation (ENSO), the Pacific Decadal Oscillation (PDO), and Closed Lows (Oakley and Redmond, 2014). Cayan (1996) studied six decades of snow course records over 11 western states and found 1 April snow water content (SWE) variations showed regional spatial coherence driven by large scale atmospheric circulation over the North Pacific/North American area. The author concluded anomalies of SWE are quite sensitive to the large-scale atmospheric circulation. Ewen et al. (2008) and Bronnimann et al. (2009) reported on a reconstruction of the PNA index from historical upper-level data back to 1922. The extended PNA index was compared with indices of the North Atlantic Oscillation, the PDO, and the ENSO. The relationship to these indices was found to be stationary over the analysis period. These results support the idea large scale atmospheric circulation in the PNA sector may remain largely constant because it is, fundamentally, a property of the Earth's size, rotation rate, heating and atmospheric depth, all of which change little. However, smaller scale events will exhibit more variability, and in many cases, may appear to occur almost randomly. McCabe and Dettinger (2002) reported on the use of SWE data to study the primary modes and the predictability of year-to-year snowpack variations in the western United States from teleconnections with Pacific Ocean climate; and, concluded examination of these complex relationships may be useful for forecasting the 1 April SWE in the western United States. Ault and St. George (2010) and St. George and Ault (2011) reported on the high variability in precipitation at decadal (10 to 20 years) or multidecadal (20 to 50 years) time scales during the last century across the central Pacific Coast of the United States (CPC). The authors made special note of a quasi-periodic function with a wavelength of 14 to 15 years but could not find a physical mechanism to explain the presence of the rhythm. Dettinger and Cayan (2014) reported the ocean-atmospheric interactions noted above are not reliable predictors of drought, i.e., some El Niño's (or warm PDO years) bring some of the wettest years to the California Delta, but others bring drought. However, the authors did note observational and tree-ring records do indicate apparent important regularities in the history of droughts in the Delta. The authors reported there is an apparent "drumbeat of drought" of 15-year duration that should be studied in more detail. Their conclusion was based on the frequency of "pineapple-express storms" making landfalls between 35N and 42.5N during each water year over the past 60 years.

Solar Effects on the Formation of the Sierra Nevada Snowpack

There is a large body of literature describing how transient properties of the sun may (or may not) affect the weather and climate patterns of Earth. Some studies propose solar variation has little or no effect whereas others suggest it is a very important component of weather and climate. A National Research Council report in 2012 titled “The Effects of Solar Variability on Earth's Climate” summarizes views and discussion points by participants of a broad scientific workshop in Boulder, Colorado. Subsequently, Phillips (2013) provided a review of the workshop report and noted while some stars exhibit dramatic pulsations that vary wildly in size and brightness, sometimes even exploding, the luminosity of our own sun varies a measly 0.1% over the course of the 11-year solar cycle. Many researchers have therefore concluded that such a small variation in the luminosity of the sun cannot be enough energy change to affect climate on earth. However, there is a growing realization among researchers that even these seemingly tiny variations may have a significant effect on terrestrial climate. Researchers have begun to wonder if something in the Pacific climate system is acting to amplify them, stating "One of the mysteries regarding Earth's climate system ... is how the relatively small fluctuations of the 11-year solar cycle can produce the magnitude of the observed climate signals in the tropical Pacific" (Phillips, 2013).

The basic problem with the above noted "amplification theory" approach is the fact that the variation of the sun’s luminosity, due to sunspots, is **NOT** the major driving force affecting Earth’s climate. The sunspot cycles do, on the other hand, represent the status of the dramatic reversal of the sun’s entire magnetic field in the short time of eleven years and records the timing of the magnetic effects the sun has on the Earth's magnetic field.

In summary, it is clear that the generation of winter precipitation in the form of snow falling on the Sierra Nevada involves many complex and interrelated processes, including, but not limited to solar effects, orbital, air/sea temperature variation, and the rotation and tilt of Earth. However, as we will demonstrate in this paper the system

complexity can be greatly simplified by observing and understanding the Sun-Earth magnetic modulation system that creates signals which are clearly detectable in the SWE time series data.

Sunspots, Solar Cycles, and the Gleissberg Cycle

There is a large collection of literature that discusses sunspots with contrasting views about who discovered them, what they represent, how they are formed, and how they may (or not) affect physical phenomena and life on Earth. Their existence was well known and reported in Ancient China and by early Islamic observers (Hathaway, 2010); however, these early naked eye observations were random, not clearly understood, and have had limited scientific value. The accuracy of counting sunspots, during each of the approximate 11 year solar cycles by westerners, was greatly enhanced when telescopes were first used to observe the sun in the early 17th century (Hathaway, 2010). From that time forward, there have been several methods developed to count and quantify sunspot numbers and relate them to the magnetic activity of the sun. The International Sunspot Number (ISSN) data base is now widely accepted and used in scientific research. Each of the 11-year sunspot cycles has been numbered starting with Solar Cycle # 1 beginning in March of 1755 to Solar Cycle #23 which ended in September of 2007. At present, we are in Solar Cycle # 24 that began in January of 2008 (Pandey et al, 2010). Hale et al. (1919) was the first to notice and report sunspots have a magnetic polarity; and, in a later breakthrough paper, Babcock (1960) proposed sunspots were an observable manifestation of the sun's magnetic properties.

It is important to note the **magnetic cycle** of the sun is not 11 years but rather it requires the sum of two sunspot cycles, which is approximately 22 years, to return to its original magnetic polarity. This cycle of the sun is named the Hale cycle after its discoverer (Hale et al., 1919). The sun, as a simplified model, can essentially be described as a sphere of rotating plasma; and because the equator of the sun is rotating faster than at the poles, magnetic flux lines are "pulled" around and stretched by the rotational difference. As the sun continues to rotate the magnetic lines are twisted into toroids. At the toroids, magnetically induced currents in the sun begin to flow and the flowing currents produce the temperature differences we observe as sunspots (Hathaway, 1998, 2010). When the sunspot activity reaches a maximum of activity the sun reverses its magnetic field. The resulting reverse currents cause a reduction of the total current flow and the number of sunspots begins to decrease with the sunspots retaining their magnetic polarity. The currents and the resulting sunspots again approach zero and the sun is once again at its maximum magnetic field strength but with a reversed magnetic polarity. The sun reverses its entire magnetic field every solar cycle of approximately 11 years and then reverses again to return to its original magnetic state after the following solar cycle. The induced currents caused by the changing magnetic field are directly proportional to the magnitude of the magnetic field and inversely proportional to the duration of the reversal. This routine reversal of the sun's entire magnetic field in the short time of 11 years has a major effect on the Earth. The induced effects on Earth by solar storm activity can also be dramatic (Love et al., 2016).

Numerous authors over many years have noted there are multi-cycle periodicities in the sunspot cycle amplitudes. Gleissberg in 1939 first noted a periodicity of seven or eight 11 year solar cycles (77 to 88 years) in the cycle amplitudes from 1750 to 1928 (Gleissberg, 1967). These amplitude variations of the solar cycles have since become known collectively as the Gleissberg Cycle (GC). Feynman and Ruzmalkin (2014) using wavelet methods reported recent extended minimums of solar and geomagnetic variability are like those which occurred in the nineteenth and twentieth centuries: 1810-1830 and 1900-1910. Similar extended minima were also evident in the period from 450A.D. to 1450 A.D. The authors argue these minima are consistent with minima of the Centennial Gleissberg Cycles (CGCs). It is important to note the authors observed a frequency merger in their data record. They found a quasiperiodic cycle beginning at about 1725 with a periodicity of about 50–60 years that drifted to lower frequencies until when at about 1850 it merged with the CGC. Since the authors were mostly interested in the period band of 80 to 110 years; and since this variation did not appear to persist, they decided to simply ignore it. Also, the authors did not discuss the 1950 frequency split reported by (Kollath and Olah, 2009). This apparent complex period variation of the GC (sunspot amplitudes) explains why so many different results for the period of the GC have been reported over the years.

Cosmic Rays and the Possible Formation and Seeding of Clouds on Earth

Galactic cosmic rays (GCRs) are energetic particles coming from outside the solar system. There have been numerous papers published over many years describing the anti-correlation between sunspot numbers (magnetic activity of the sun) and the modulation of GCRs (Forbush, 1954). Pandey et al. (2013) noted the number of sunspots indicates the level of solar activity. Falayi and Rabiu (2012) and Chowdhury et al. (2013) reported on the interrelationship between the monthly means of time derivatives of the Earth's horizontal geomagnetic field (dH/dt),

sunspot number (SNN), and the aa index. The aa index being a measure of the disturbance level of the Earth's magnetic field. The authors concluded that as sunspot numbers increase the base level of Earth's geomagnetic activity also increases adding to the deflection of GCRs.

GCRs are thought to affect atmospheric properties on Earth via ionization/radiation. However, the role of ionization in atmospheric processes by GCRs has been a controversial matter since it was first suggested fifty years ago (Ney, 1959) and (Dickenson, 1975); and, later detected through correlation between global cloud cover and the influx of GCRs (Svensmark et al., 1997). The cosmic rays are thought to affect cloud formation on Earth by creating condensation nuclei (Knivetun & Todd, 2001), (Enghoff et al., 2011). However, correlations between GCR variations and changes in aerosol counts and cloud properties in the atmosphere, are disputed, (Calogovic et al 2010), (Kulmala et al., 2010), and (Svensmark et al., 2000, 2006, 2013). However, Yu and Luo (2014) and Svensmarl et al. (2016) have recently provided additional support for the inferred linkages between cosmic rays and clouds on Earth. They propose the Sun's changing magnetic field has an influence on GCRs, with a stronger magnetic field deflecting more cosmic rays and a weaker one allowing more into the solar system.

DATA AND METHODOLOGY

We investigated, using wavelets, several long-term snow water equivalent (SWE) records in the Sierra Nevada and found linkages between sunspots (i.e., the magnetic activity of the sun), GCR intensity, and SWE. It is important to note the 11 year and 22-year visible sunspot cycles are **NOT** found in the SWE data, but rather, we found evidence of a Sun-Earth magnetic carrier suppressed amplitude modulation system that modulates the formation of the Sierra snowpack resulting in the generation of four signals.

Snow Water Equivalent Data in the Sierra Nevada

From 1905 to 1915, the pioneer of snow sampling, Professor J.E. Church of the University of Nevada, Reno, invented a snow pack sampling methodology and established a system of snow courses at Mt. Rose and within the Lake Tahoe Basin, Figure 1. This included a sampling site established at Lake Lucille in the Fallen Leaf Lake watershed in 1913 (Werner, 2006). Church developed his Mt. Rose snow sampler to accurately measure the water content of a snowpack.

The SWE data in the Sierra Nevada we used for this paper were taken from the 100-year long records of annual SWE measurements taken by hand at several of Church's original sampling sites plus one site farther to the south. Representative sites were selected based on the length of their records and proximity to the Sierra Nevada crest, where April 1st snowpack is generally greatest. For example, the SWE recorded at Mt Rose (19K02) is one of the longest continuous SWE records available (1910-2017) in the United States.

Spectral Analysis

Among all the spectral analysis tools used in frequency analysis, the most commonly applied is the Fourier transform. Although the Fourier transform is efficient and robust for analyzing the frequency content of a periodic signal over an entire time record, it is limited in its ability to detect changes in frequency as a function of time. The Morlet Wavelet transform, on the other hand, can capture the short duration, high frequency, as well as the long duration, low frequency information simultaneously (Torrence and Compo, 1998). For example, Figure 2, shows the

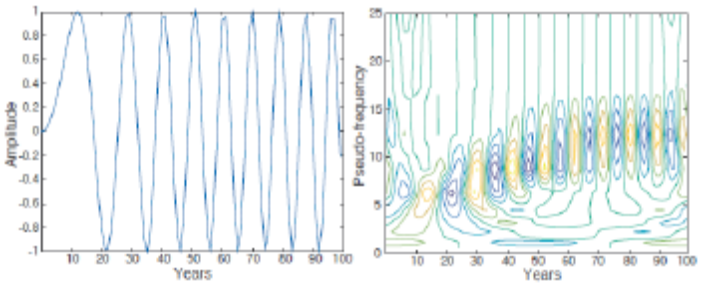

Figure 2. (a) Example of a frequency modulated sine wave defined as y = (sin(2*pi*0.1*t.*k)) and k=(1.0-exp(-t*0.02)) and (b) the application of the Morlet Transform (a).

Morlet Transform applied to a time varying periodic signal where it becomes straightforward to observe the time-varying frequency content. SWE data were analyzed using both Fourier Transform and Morlet Wavelet Transform methods. The SWE data were de-trended and passed through an anti-aliasing, second-order Butterworth low-pass filter with a cutoff period of 3.3 years. The sampling rate was chosen to satisfy the Nyquist rate of at least 2 times the highest frequency content in the SWE data records. Because the SWE data have relatively few samples (~100 measurements or less), it was necessary to apply a Hamming window to the data prior to applying the short record FFT and/or the Morlet Transforms. Furthermore, the frequency (or period) resolution is relatively coarse since resolution is a function of the inverse of the time record length. These approaches were applied to the SWE time series data for Lake Lucille (LLSWE), Ward Creek#2 (WCSWE), and Mt. Rose (MRSWE) for the period 1913 to 2014, then again over the period 1928 to 2014 for consistent comparison with results from the Mammoth Pass site (MPSWE).

Sunspots During the Partial Water Year (October 1 to March 31)

We used the revised Version 2.0 monthly International Sun Spot Number (ISSN) data for our analysis from the World Data Center SILSO, Royal Observatory of Belgium, Brussels. The (ISNN) record has been divided into 24 cycles starting with Solar Cycle #1 beginning in 1755 and continuing up to the present Solar Cycle 24. (Figure 3a) shows a traditional plot of the smoothed annual sunspot record from 1755 to 2007 (Solar Cycles 1 to 23). The traditional plot of sunspots displays the dominant Schwab Cycle of 11 years (Hathaway, 2010), Figures 3a, b, c, but does not account for the magnetic polarity of the sunspots.

The first step in our analysis was to reconstruct the ISSN time series data to account for the reversal of the sun's magnetic field every 11 years. This procedure resulted in a modified sunspot record with a Solar cycle period of approximately 22 years (two conventional sun cycles) Figures 3d, e, f. A close look at Figure 3d shows the start of the period for Solar Cycles 15 to 23 begins in WY 1914 and ends in WY 2007.

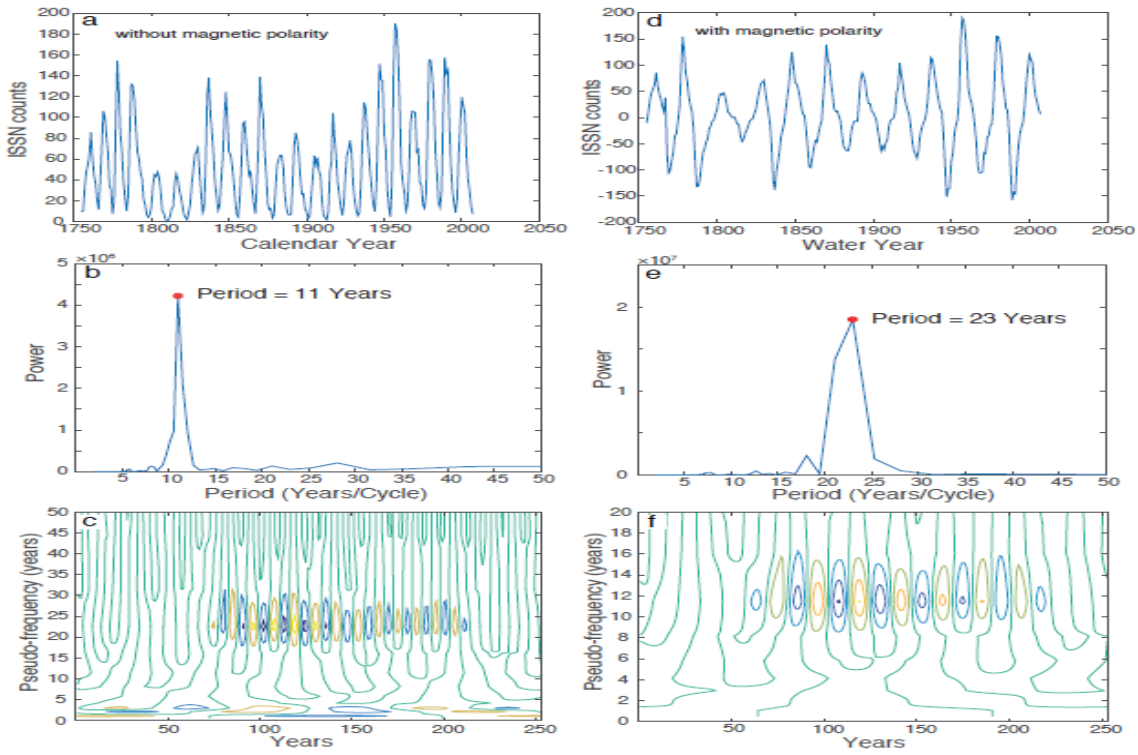

Figure 3. (a) A typical plot of the International sunspot numbers (ISSN) for Solar Cycles 1 to 23 (1755 to 2007). (b) A plot of the Fast Fourier Transform (FFT) of the ISSN sunspot time record shown in (a). (c) The Morlet Wavelet transform of the ISSN sunspot time record shown in (a). (d) Plot of the sunspot cycle time series that includes magnetic polarity. (e) Result of the Fast Fourier Transform (FFT) applied to (d). (f) The Morlet Wavelet transform applied to (d). Note the dominant period of the modified sunspot cycle is now ~23 years (i.e., the Hale Cycle).

It is important to note, the traditional sunspot record can be obtained from our modified sunspot record by simply passing our modified sunspot record through a full wave rectifier, or in other words, by simply taking the absolute value of our modified sunspot record.

The traditional ISSN time series was then converted from calendar year to partial Water Year to match the timing of the Sierra Nevada snowpack measurements (October 1st to March 31st). We denote the modified series as ACWYSSN. As with the SWE data, the ACWYSSN time series was analyzed using the same Fourier and Morlet Wavelet Transform methods described earlier. The ACWYSSN data were de-trended by subtracting the mean (or a best-fit line in the least-squares sense) from the data. The sunspot data were passed through an anti-aliasing, second-order Butterworth low-pass filter with a cutoff period of 3.3 years. The sampling rate was chosen to satisfy the Nyquist rate of at least two times the highest frequency content in the ACWYSSN data records. Because the ACWYSSN time series has relatively few samples (~100 measurements or less), it was necessary to apply a Hamming window to the data prior to the short record FFT and Morlet Transform. The frequency (or period) resolution is relatively coarse since time and frequency resolution is a function of the inverse of the record length.

Development of an Amplitude Modulation Model for the Generation of SWE.

The mathematical basis of our model is described in equations [1] and [2]. In words, our hypothesis is, the snowpack (SWE) in the Sierra Nevada is being created by a carrier suppressed amplitude modulation process involving the multiplication of three signals, the first being a statistically independent "carrier" signal being generated by the Earth's atmospheric circulation parameters including orbital (inclination, eccentricity, precession, obliquity, and rotational), depth of the atmosphere, and heating by the sun; the second signal being generated by the frequency of the reversal of the sun's magnetic field; and, the third signal being due to the time varying amplitude of the sun's magnetic field represented by GC.

It is well known the multiplication of two sinusoids results in the creation of a process consisting of the sum and difference frequencies of a "carrier signal" frequency and a "modulating signal" frequency (Gruber, 1992), (Mathys, 2014). Amplitude modulation, for example, is used to translate low frequency audio signals into high frequency radio signals so the radio signals can be transmitted over long distances. At the receiver end, the high frequency radio signals are then demodulated resulting in the recovery of the original low frequency audio signals.

Our modulation model involves the multiplication of three signals which generates another level of sum and difference frequencies and hence four signals are generated instead of just two. One of the standard demodulation methods for a carrier suppressed amplitude modulation process is to simply multiply the received signal by the transmitted carrier signal. For our three-signal model, we can demodulate the modulated signal by multiplying the modulated signal by any two of the three modulating signals. This method does require knowledge of the frequency and phase of the modulating signals. However, if this information for the modulated signal is not known, it can be estimated from the modulated signal.

Our model can be mathematically described as follows. We assume the Sierra Nevada snowpack SWE_m is being generated as the result of a carrier suppressed amplitude modulation of three signals, fc, fs, and fg where:

$fc = K_c \sin(\Theta_c)$ = carrier signal (Earth signal)= fc

$fs = K_s \sin(\Theta_s)$ = modified sunspot signal =ACWYSSN

$fg = K_g \sin(\Theta_g)$ = time varying Gleissberg Cycle signal = GC

This three-signal multiplication process produces a modulated signal (SWE_e) with the four frequencies as noted above. The Earth carrier frequency is not separately present in the carrier suppressed modulated signal. The mathematical representation of this amplitude modulation process is shown below in equation [1], where the product-to-sum trigonometric identity is used.

The estimated SWE_e is determined using by the multiplication of the three signals fc ,fs ,and fg .

$$SWEe = K_c \sin(\Theta_c) \times K_s \sin(\Theta_s) \times K_g \sin(\Theta_g)$$

$$= K[\sin(\Theta_c - \Theta_s + \Theta_g) + \sin(\Theta_c + \Theta_s - \Theta_g)] \quad [1]$$

$$- K[\sin(\Theta_c - \Theta_s - \Theta_g) + \sin(\Theta_c + \Theta_s + \Theta_g)]$$

Where $K = K_c K_s K_g/4$ and $\Theta_c > \Theta_s > \Theta_g$

$$\Theta_n = \omega_n t + \Phi_n = 2\Pi f_n t + \Phi_n$$

Φ_n = phase of Θ_n

It is noted, in the above process, the multiplication of the three signals of frequency fc, fs and fg results in the generation of four signals which we will denote as f_1, f_2,f_3,and f_4.

It is possible to arrange these operations in the tabular form shown below for easy analysis. The T_n are the respective periods calculated as the inverses of each f_n:

$$\begin{aligned} f_{1=1/T1} &= fc + fs + fg \\ f_{2=1/T2} &= fc + fs - fg \\ f_{3=1/T3} &= fc - fs + fg \\ f_{4=1/T4} &= fc - fs - fg \end{aligned} \quad [2]$$

The solution of equation [2] provides a starting value for fc in our modulation model. We first multiply fc times the modified sunspot record ACWYSSN, and then multiply this product by the time series GC. The result of this multiplication produces an estimated value, SWEe. The model then calculates the cross-correlation coefficient between the measured values, SWEm, and the estimated values, SWEe, and applies iteration methods to adjust the model parameter f_c, to maximize the correlation coefficient.

RESULTS

The first step in the analysis of the SWE was to compare the spectral content from several spatially separated Sierra Nevada snow course sites. The Lake Lucille sampling site and the two other nearby sites, Ward Creek #2 (20K17) and Mt. Rose (19K02), were selected as representative sites for the Lake Tahoe region. The fourth site, farther south, was established in 1928 at Mammoth Pass (LADWP-205). The Mammoth Pass snow course provided a continuous 86-year record from a more distant location, but still within the same U.S. Climate Division as the other three sites (Nevada 1 and California 3, Russel, et al (2014).

The spectral calculations for the water year period 1928 to 2014 (Figure 4) reveals a nearly identical peak period of 14.5 years, and a second peak at a period of ~32 years, a third peak with a period of 7.9 and a fourth more subtle peak at a period of ~6 years for the four Sierra Nevada SWE sites. The longer record of SWE data for the period 1913 to 2014 at Lake Lucille, Ward Creek, and Mt. Rose shows the four peaks more clearly, see Figure (6).

Cross correlation estimates yielded correlation coefficients of 0.88 (Table 1), suggesting the SWE spectral content is highly correlated over a broad area of the northern to central Sierra Nevada. The use of the Morlet Transform allowed us to observe a shift in the 14.5-year period in the SWE data that was not observable using standard FFT analysis. The reason for this shift will be discussed later in this paper.

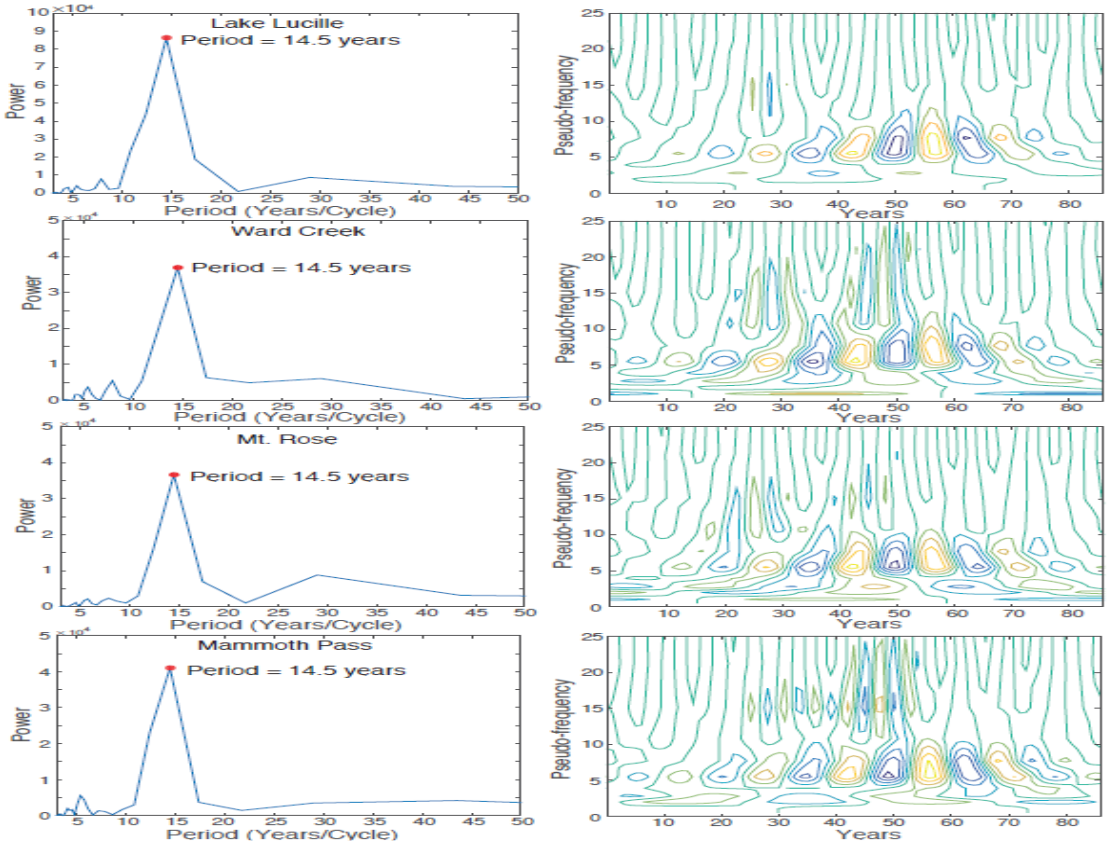

Figure 4. Comparison between Snow Water Equivalent spectral responses for the time 1928–2014. Panels in the left-hand column are results of the Fast Fourier Transform, right-hand columns show the Morlet Wavelet Response. (a and b) Lake Lucille; (c and d) Ward Creek; (e and f) Mt. Rose; (g and h) Mammoth Pass. It is possible to detect the frequency shift of the major spectral peak during the time record using the wavelet approach.

Table 1. List of snow courses showing the high correlation between the snow course SWE data for sites in the U.S. climate zones Nevada #1 and California #3 in the Sierra Nevada.

Name	Station ID	Location LAT/LONG	Elevation (m)	Climate region	Period of data	Correlation with LLSWE
Lake Lucille	20L04	38.96/-120.11	2,496	CA-3	1913-2014	1.00
Ward Creek #3	20K17	39.14/-120.23	2,164	CA-3	1913-2014	0.88
Mt Rose	19K02	39.35/-119.88	2,743	NV-1	1913-2014	0.88
Mammoth Pass #	LADWP(205)	37.61/-119.03	2,835	CA-3	1928-2014	0.89

The next step in the analysis was to apply our model to determine how well we could reconstruct the Sierra Nevada SWE from the multiplication of the carrier signal, fc, the water year corrected sunspot series ACWYSSN, and GC. Referring to Equation (1), the three inputs to the model are the carrier signal ,fc, the modified sunspot number time series, fs=AWYCSSN, and the time varying GC. The GC for the period 1917 to 2014 represents the amplitudes of the YSSN sunspot record over the period 1917 to 2014. We used an appropriate curve fitting routine

to fit the amplitude points in Figure 5. It can be seen the resulting time variable curve fit for the GC, which has a correlation coefficient of 0.72, is quite good. We then used the resulting time series as the GC signal for our analysis.

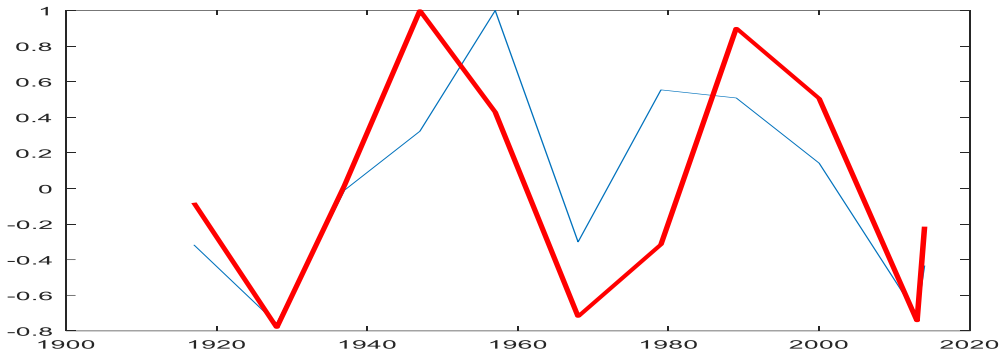

Figure 5. Time varying curve fit for the Gleissberg Cycle from 1917 to 2014

As an example, the Mt. Rose SWE spectral data record over the time period of Solar Cycles 15 to 23 (WY1914 to WY2007) is shown in Figure 6. Apply equations [1] and [2] to determine the starting value for the carrier, fc.

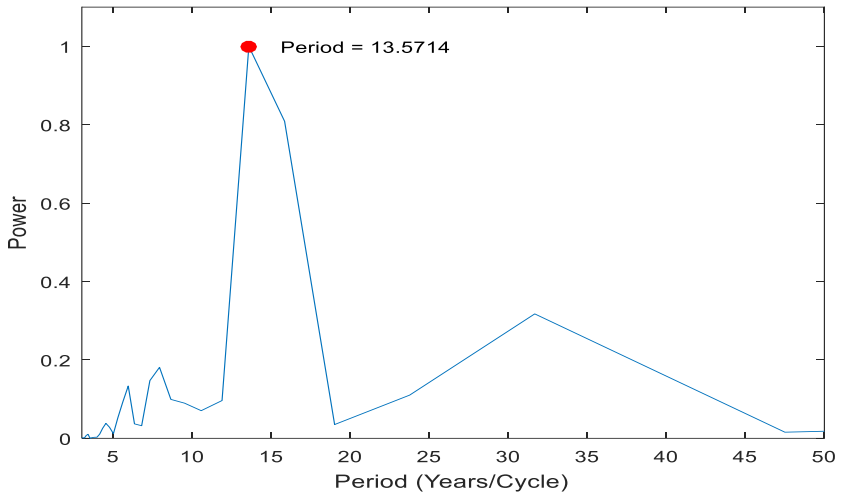

Figure 6. A plot of the Mt. Rose SWE data from WY1914 to WY2007

The spectral signatures of the four signals in the SWE data record are found to be T1=5.9375, T2= 7.9167, T3= 13.5714, and T4= 31.6667. In terms of frequencies, these values are f1 = 0.168421, f2 = 0.126315, f3 = 0.0.073684, and f4= 0.031579. The values for fc, fs, and fg are then found by applying equation [2]:

$f_1 = fc + fs + fg = 0.168421$ with $T_1 = 5.9375$
$f_2 = fc + fs - fg = 0.126315$ with $T_2 = 7.9167$
$f_3 = fc - fs + fg = 0.073684$ with $T_3 = 13.5714$
$f_4 = fc - fs - fg = 0.031579$ with $T_4 = 31.6667$

The solution is found to be fc= 0.10000 (Tc= 10.0), fs= 0.047368 (Ts= 21.1),and fg= 0.021053 (Tg= 47.5). The value fc =10.0,is used as the starting value for our model.

An example model output for the Lake Lucille SWE data, LLSWE, and its comparison to the measured LLSWE data record over the period WY 1916 to WY 2007 is shown in Figure 7. It is very important to note the spectral shift of the major "drought buster" (El Niño) peak (15.3) shown in the wavelet record of Figure 7-a. The peak period shifted from 16 years to 12 years over the 91 year SWE data record from 1916 to 2007. This is a period shift of approximately 0.044 years per year. The shift is generated by the time varying Gleissberg Cycle. Notice the

effects caused by the apparent frequency split of the Gleissberg Cycle around 1950 as reported by Kollath & Olah (2009). This is clearly seen in the SWE data and was picked up by the model. The correlation coefficient between the measured SWEm and the estimated SWEe was 0.81 for this example. The average period between the El Niño peaks is getting shorter meaning more frequent Atmospheric Rivers are to be expected during upcoming winters.

The Oceanic Niño Index (ONI) has become the de-facto standard that NOAA uses for identifying El Niño (warm) and La Niña (cool) events in the tropical Pacific. It is interesting to investigate, using our model, the most recent running 3-month mean sea surface temperature (SST) data available for El Niño (warm) and La Niña (cool) in the Niño 3.4 region i.e., 5ºN-5ºS, 120º-170ºW.

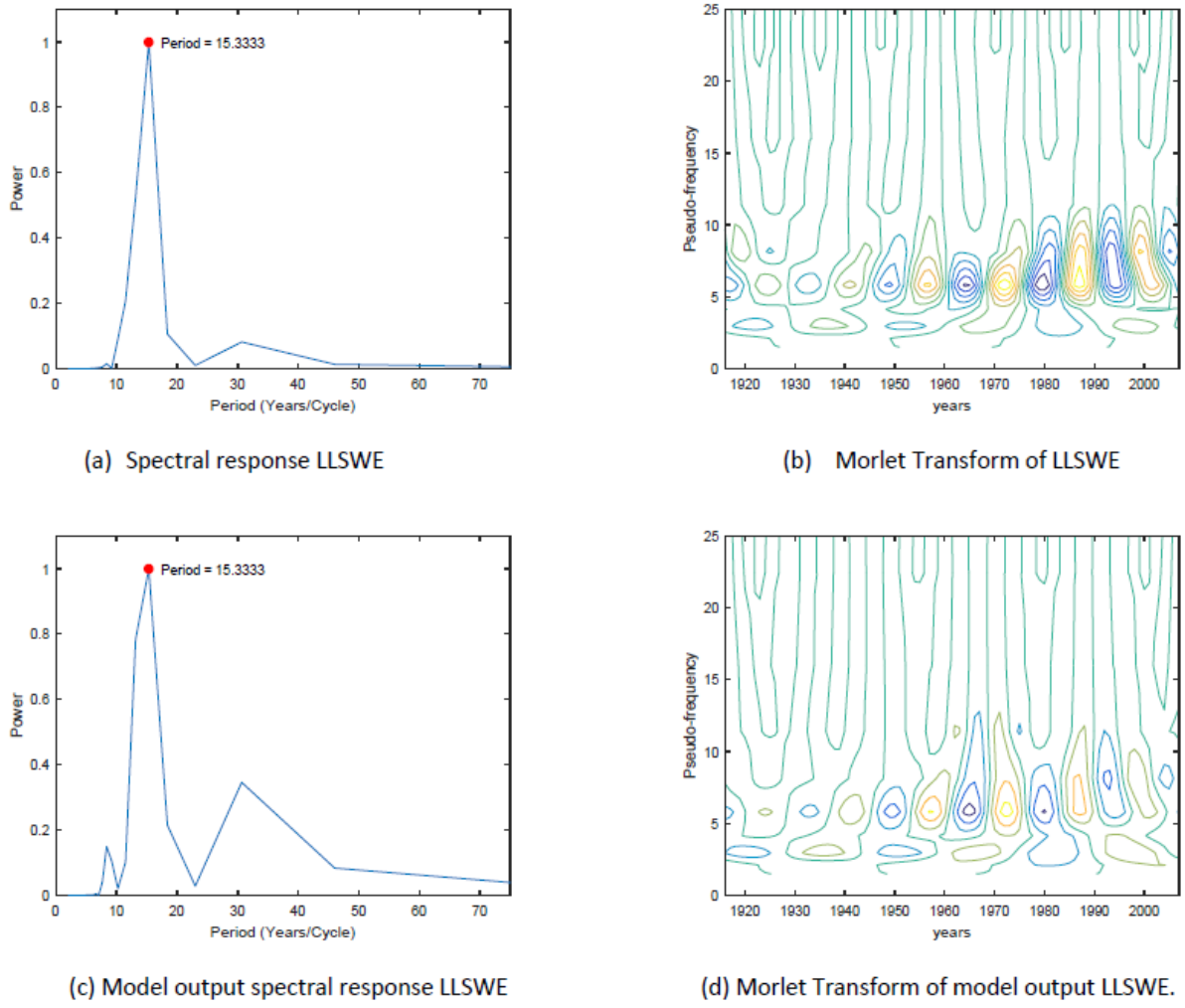

Figure 7. (a) Lake Lucille measured SWE data for the period WY1916 to WY2007, (b) Morlet Transform of Lake Lucille data, (c) Output of the model with a correlation coefficient of 0.81 to the measured SWE data, and (d) Morlet Transform of model output for Lake Lucille.

Figure 8 presents a comparison between the spectral content of the ONI converted to WY and the spectral content of the Mt. Rose SWE data over the period WY1951 to WY2016.

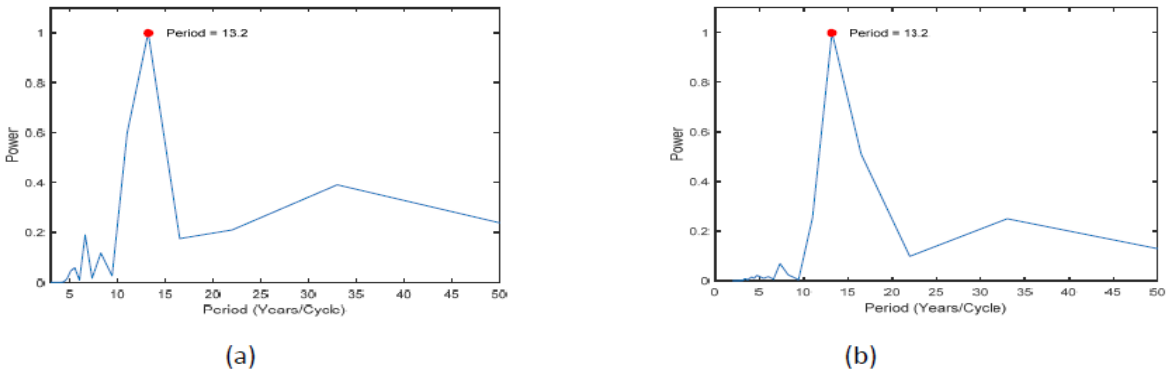

Figure 8. Spectral record of (a) MT. Rose SWE and (b) the Oceanic Niño Index (ONI) from WY 1951 to WY 2016.

Several other snow courses located in the Western United States, with long historical records, were investigated using our same approach. Our model was applied to several climate regions including the Rocky and Cascade Mountains. The analysis of the data from these additional snow courses show similar solar forcing on SWE records, but with a different carrier frequency, f_c, the results from this extended investigation will be reported in a later paper.

DISCUSSION AND CONCLUSIONS

The spectral content of the SWE data and the high correlation coefficients amongst the sites listed in Table 1.0 suggest the Sierra Nevada snowpack variability is not a function of individual watersheds and/or local topographic relief, but rather a representation of broad-scale climatic phenomena affecting the entire Sierra Nevada. Since the generation of precipitation falling onto the Sierra Nevada involves many complex and interrelated factors including, but not limited to, effects due the Earth's orbital (including rotation and tilt) properties, air and sea temperatures, solar effects (magnetic and insolation), it is interesting to see how these very complex processes can be lumped into a simple model. The complex process can be modeled using a suppressed carrier amplitude modulation process. This process involves the multiplication of three signals, the first being an Earth statistically independent "carrier" signal, fc, being generated by the Earth's large scale atmospheric circulation parameters, the second, the Water Year modified sunspot cycle, fs , and the third, the Gleissberg Cycle ,fg. It is important to note since the Earth's carrier signal remained constant over the period of our analysis (nearly 100 years) this supports the fact large scale atmospheric circulation remained nearly constant in the areas we studied.

It is important to note the quasi-periodic function with a wavelength of 14 to 15 years reported by St. George and Ault (2011) without a physical mechanism to explain the presence of the rhythm; and, the approximate average "drumbeat "of the 15 year period in the 60-year data record, cited by Dettinger and Cayan (2014), is the variable peak period we found in the highly correlated SWE data analyzed from Table 1 and shown in Figure 7. We conclude the "drought buster" El-Niño cycle is changing to a shorter period in response to changes of the Gleissberg Cycle at a rate of approximately 0.044 years per year.

We needed to reverse the phase of the GC curve, gc, by 180 degrees, to produce the highly correlated SWEe to SWEm results. This is an important observation and supports the idea it is highly likely the anti-correlation GCRs may be the mechanism responsible for the connection between the magnetic activity of the sun (sunspots) and the SWE.

Based on the results presented in this paper, we conclude the major driving forces of winter precipitation, in the form of snow, in the northern and central Sierra are the reversal of the sun's magnetic field and a statistically independent "carrier" signal being generated by the Earth's large scale atmospheric circulation parameters.
This work can be extended to include the study of past droughts by reconstructing the sunspot record accordingly.

ACKNOWLEDGEMENT

We thank the WDC-SILSO, Royal Observatory of Belgium, Brussels for use of their data bank for our sunspot numbers.

REFERENCES

Ault, T.R. and S. St. George. 2010. The magnitude of decadal and multidecadal variability in North American precipitation. Journal of Climate Vol. 23, 842- 850.

Babcock, H.W. 1961. The topology of the Sun's magnetic field and the 22-year cycle. Astrophysical Journal, Vol. 133, *572–587.*

Bronnimann, S., et al. 2009. Variability of large scale atmospheric circulation indices for the northern hemisphere during the past 100 years. Meteorogische Zeitschrift, Vol. 18(4), 379-396.

Calogovic J., et al. 2010. Sudden cosmic ray decreases: No change of global cloud cover. Geophysical Research Letters, Vol. 37, L03802, 1-5

Cayan D. R. 1996. Interannual climate variability and snowpack in the Western United States. Journal of Climate, Vol.9, 928- 948.

Chowdhury P. et al. 2013. Heliospheric modulation of galactic cosmic rays during Solar Cycle 23. Solar Physics. Vol 286,577-591.

Dettinger M., and D. Cayan. 2014. Drought and the California Delta- A matter of extremes. San Francisco Estuary & Watershed Science, 1-6.

Dickenson R.E. 1975. Solar variability and the lower atmosphere. Bulletin American Meteorological Society Vol. 56(12), 1240- 1248.

Enghoff, M. B. et al. 2011. Aerosol nucleation induced by a high-energy particle beam. Geophysical Research Letters. Vol. 38, L09805, 1-4.

Ewen, T., et al. 2008a. An extended Pacific North American index from upper air historical data back to 1922. Journal of Climate Vol. 21, 1295–1308.

Ewen, T., et al. 2008b. A monthly upper-air dataset for North America back to 1922. The Monthly Weather Review, 136, 1792–1805.

Falayi , E.O.& A. B. Rabiu . 2012. Dependence of time derivative of horizontal geomagnetic field on sunspot number and aa index. Frontiers in Science, Vol. 2(1), 1-5.

Feynman J. & A. Ruzmalkin. 2014. The centennial Gleissberg Cycle and its association with extended minima. Journal of Geophysical Research: Space Physics, 6027- 6041

Forbush, S.E. 1954. World-wide cosmic-ray variations, 1937-1952. Journal of Geophysical Research, Vol. 59, 525-542.

Gleissberg, W. 1967. Secularly smoothed data on the minima and maxima of sunspot frequency. Solar Physics, Vol. 2,231-233.

Gruber, M. 1992. Synchronous detection of am signals. QEX (127), September, 9-16.

Hale G.E., et al. 1919. The magnetic polarity of sunspots. The Astrophysical Journal, Vol. 49, 153–178.

Hathaway, D. H. 1998. The solar dynamo, American Geophysical Union, special editions. From the Sun: Auroras, Magnetic Storms, Solar Flares, Cosmic Rays, ISBN: 978-0-87590-292-0, Vol. 50, 113- 122.

Hathaway, D. H. 2010. The solar cycle. Living Reviews Solar Physics, Vol. 7(1), 1-65.

Knivetun, D. R. and M. C. Todd. 2001. On the relationship of cosmic ray flux and precipitation. Geophysical Research Letters, Vol. 28(8), 1527-1530.

Kollath Z. and K. Olah. 2009. Multiple and changing cycles of active stars. 1. Methods of analysis and applications to the solar stars. Astronomy & Astrophysics, Vol. 501, 695 – 702.

Kulmala, M. et al. 2010. Atmospheric data over a solar cycle: no connection between galactic cosmic rays and new particle formation. Atmospheric Chemistry & Physics, Vol. 10, 1885-1898.

Mathys, P. 2014. Lab 7: Amplitude modulation with suppressed carrier. ECEN 4652/5002 Spring 2014, Electrical, Computer & Energy Engineering Department, University of Colorado,1-15.

McCabe, G. J. and M. D. Dettinger. 2002. Primary modes and predictability of year-to -year snowpack variations in the Western United States from teleconnections with Pacific Ocean climate. Journal of Hydrometeorology, Vol. 3, 13- 25.

Ney, E. P. 1959. Cosmic radiation and the weather. Nature 183(4659), 451-452

Oakley, N. S. and K. T. Redmond. 2014. A climatology of 500-hPa closed lows in the Northeastern Pacific Ocean. 1948-2011, Journal of Applied Meteorology and Climatology, Vol. 53, 1578- 1592.

Pandey, S. K., et al. 2010. Study of sunspots and sunspot cycles 1-24. Current Science, Vol. 98(11), 1496- 1499.

Pandey, U. et al. 2013. Correlative analysis of long term cosmic ray variation in relation with sunspot number. Advances in Physics Theories and Applications, Vol. 22, 10 – 13.

Phillips, T. 2013. "The Effects of Solar Variability on Earth's Climate," NASA workshop ISBN: 978-0-309-26564-5.

St. George and T.R. Ault. 2011. Is energetic decadal variability a stable feature of the central Pacific Coast's winter climate? Journal of Geophysical Research, Vol. 116, D12102, 1-6.

Svensmark, H. and E. Friis-Christensen. 1997. Variation of cosmic ray flux and global cloud coverage- a missing link in solar-climate relationships. Journal of Atmospheric and Solar-Terrestrial Physics, Vol. 59(11), 1225-1232.

Svensmark, H. and E. Friis-Christensen. 2000. Reply to comments. Journal of Atmospheric and Solar-Terrestrial Physics, Vol. 62, 79-80.

Svensmark, H. et al. 2006. Experimental evidence for the role of ions in particle nucleation under atmospheric conditions. Proceedings of the Royal Society A., Vol. 463, 385 – 396.

Svensmark, H. et al. 2013. Response of cloud condensation nuclei (> 50nm) to changes in ion-nucleation. Physics Letters A.,Vol. 377, 2343-2347.

Svensmark, H. et al. 2016. The response of clouds and aerosols to cosmic ray decreases. Journal of Geophysical Research: Space Physics, Vol. 121(9), 8152 – 8181.

Torrence, C. and G. P. Compo. 1998. A practical guide to wavelet analysis. Bulletin of the American Meteorological Society, Vol. 79(1), 61-78.

Werner, J. 2006. Snow survey centennial celebration 1906 – 2006. Snow Survey & Water Supply Forecasting Program January 9, 2006, 1-3.

YU, F. and G. Luo. 2014. Effect of solar variations on particle formation and cloud condensation nuclei. Environmental Research Letters, Vol. 9(4), 1-7.